16th World Conference on Earthquake, 16WCEE 2017
Santiago Chile, January 9th to 13th 2017
Paper N° 2437
Registration Code: S-H1463282038

SEISMIC BEHAVIOUR OF METAL DUCT CONNECTIONS IN PRECAST CONCRETE PANELS

P. Seifi[(1)], R. S. Henry[(2)], J. M. Ingham[(3)]

[(1)] PhD Candidate, Department of Civil and Environmental Engineering, University of Auckland, psei698@aucklanduni.ac.nz
[(2)] Senior Lecturer, Department of Civil and Environmental Engineering, University of Auckland, rs.henry@auckland.ac.nz
[(3)] Professor, Department of Civil and Environmental Engineering, University of Auckland, j.ingham@auckland.ac.nz

Abstract

The seismic performance of grouted connections between precast concrete panels was questioned in New Zealand following the 2010/2011 Canterbury earthquakes. Inadequate connection detailing contributed to the failure of some panel connections, and recommendations for more robust detailing of grouted metal duct connections were published by the Structural Engineering Society of New Zealand. In the research reported here a set of experimental tests was conducted in order to evaluate the seismic behaviour of both previously used detailing and of currently-recommended detailing of precast concrete walls with grouted metal duct connections. A total of seven full-scale precast concrete walls were subjected to reverse cyclic in-plane lateral loading. The geometry and reinforcement detailing of the walls was based on a review of over 4800 constructed precast concrete panels in order to test realistic panel detailing. Various parameters such as the wall thickness, aspect ratio, axial load, number of layers of reinforcement, and the use of transverse reinforcement around the connections were included in the experimental programme. The tests confirmed that in-plane wall response was dominated by connection behaviour, with significant rocking at the wall-to-foundation interface. Failure was typically controlled by fracture of the vertical reinforcement at the connection. The existing connections performed adequately when subjected to in-plane cyclic loads, but performance was found to diminish as the axial load and the wall dimensions increased. The use of transverse confinement reinforcement around the grouted metal ducts was observed to improve the robustness of the reinforcement splice at large lateral drifts.

Keywords: Precast concrete; Shear wall; metal duct connection; lateral cyclic loading.

1. Introduction

Since the 1960s there has been significant use of precast concrete for a variety of structural components including walls, floor systems, moment resistant and gravity load frames, and cladding panels [1]. Many buildings are constructed using precast concrete because of advantages that include an increased speed of construction, optimised material consumption, reductions in on-site labour work, and improvements in quality control [2]. In New Zealand, precast concrete walls have been widely used in building construction, from low-rise structures such as warehouses to multi-storey buildings. The large strength and stiffness of precast concrete walls against both vertical and lateral loads allow them to be used as a primary force resisting system.

One method for connecting precast concrete walls to the foundation is to use grouted metal duct connections. This method consists of metal ducts that are placed inside the wall during casting and then connection bars from the foundation are placed inside the ducts during site installation, with the ducts then filled with non-shrink grout. In thin panels, metal duct connections may exhibit non-ductile behaviour when the concrete from around the connection spalls, leading to the metal duct being pulled out from the wall. From 2011 onwards the Structural Engineering Society of New Zealand (SESOC) [3] has recommended the use of connection confinement by placing additional longitudinal bars and closed stirrups around each duct to alleviate this problem, as shown in Figure 1.

An experiment programme was designed and conducted to evaluate the seismic performance of wall-to-foundation grouted metal duct connections with both existing and the proposed new detailing. The geometry and

reinforcement of the test walls and their connections with the foundation were based upon a review of 4800 collected panel details from three major New Zealand cities (Auckland, Wellington, and Christchurch).

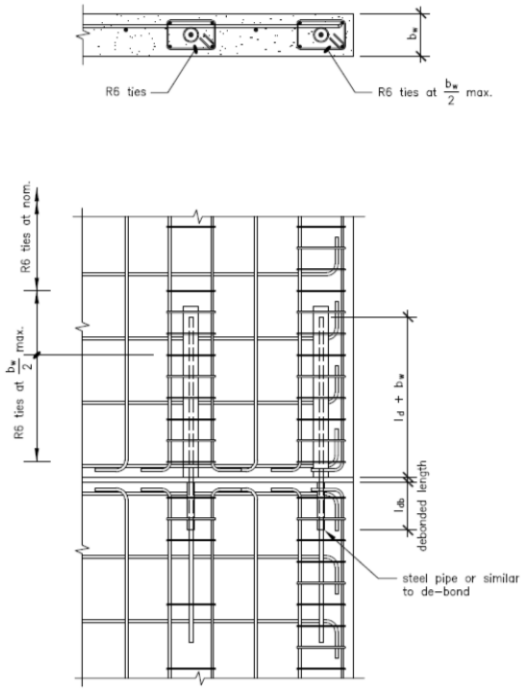

Fig. 1 – Proposed metal duct detailing. [4]

2. Precast panel survey

A review of manufactured precast concrete panels was conducted in order to understand commonly used detailing of precast concrete walls and their connections. More than 4800 precast concrete panels detailing from 108 different buildings was collected and reviewed from three major New Zealand cities of Auckland, Wellington and Christchurch. The geometry of the panels, reinforcement of connections and panels, and type of the connections were reviewed and categorized [4].

The most commonly documented panel configuration had a 150 mm thickness and was reinforced with a single layer of longitudinal bars (42% of all panels), whilst double layer reinforced panels with a 200 mm thickness were observed in 25% of the reviewed detailing. Panel reinforcing typically consisted of HD12 bars (d_b = 12 mm, f_y = 500 MPa) spaced at 250 mm in both the horizontal and vertical directions. In panels with a 200 mm or greater thickness, double layers of HD12 bars spaced at 250 mm were used in most cases. The most commonly used reinforcement content for metal duct connections between the wall and foundation was between 0.4% and 0.6% of the gross wall section. In most metal duct connections a 16 mm diameter bar was used for the connection reinforcement (HD16) with a spacing of 400 mm to 450 mm.

3. Experimental Programme

An experimental programme was developed to examine the seismic behaviour of precast concrete structural walls connected to their foundation using grouted metal duct connections. Different parameters such as magnitude of axial load, panel reinforcement, aspect ratio of the panels, panel thickness and use of the proposed confining stirrups were included in the experimental programme

3.1 Test specimen details

The geometry and reinforcement of the test panels were selected according to the reviewed panel detailing in order to examine the behaviour of panels with the most commonly used detailing used in New Zealand. All test panels were designed to have a dominant flexural and/or rocking behaviour as this type of design was more

commonly used in the reviewed detailing. The dimensions and reinforcement details of the test panels and the applied axial load are summarised in Table 1. The first two panels represented perimeter walls in industrial warehouse buildings, with an aspect ratio of 3 and a low level of applied axial load. Panel 3 had a same geometry as Panel 1 but with axial load applied. Panel 4 and Panel 5, which represented walls in multi-storey buildings, had an aspect ratio of 2 with a moderate axial load. All panels except Panel 2 had a 150 mm thickness, and were vertically reinforced with a single layer of HD12 reinforcement spaced at 225 mm. Panel 2 had a 200 mm thickness and had a double layer of HD12 reinforcement spaced at 225 mm. In all panels both the vertical and horizontal panel reinforcement was anchored at the edges of the panel with a 90° standard hook.

For connecting the panel to the foundation, starter bars from the foundation were embedded inside 600 mm long metal ducts that were later filled with non-shrinkage grout. The other end of the connection reinforcement was anchored inside the foundation by a 90 degree standard hook. The wall panel was initially erected on top of the foundation by providing 20 mm gap underneath the wall. The area around the gap was dry-packed and a day later was filled by pumping non-shrinkage grout into the metal ducts.

Table 1 – Properties of the test panels

Test number	Length (mm)	Height (mm)	Aspect ratio	Thickness (mm)	Connection reinforcement	Vertical reinforcement	Confining reinforcement	Axial Load (%Agf'c)
1	1000	3000	3	150	HD16@400	Single layer HD12@225	-	0
2	1000	3000	3	200	HD16@400	Double layer HD12@225	-	0
3	1000	3000	3	150	HD16@400	Single layer HD12@225	-	5%
4	2000	4000	2	150	HD16@450	Single layer HD12@225	-	5%
5	2000	4000	2	150	HD16@450	Single layer HD12@225	Rectangular	5%

3.2 Material properties

Samples of the steel reinforcement, concrete, and grout were taken during the construction of the panels and during grouting of the connections. The reinforcement samples were tested by applying monotonic axial tensile loads to the samples. For each experiment three concrete compression tests were performed on cylinder samples with a radius of 100 mm and height of 200 mm. In addition three grout cube samples with dimensions of 50×50×50 mm were tested for each panel. Concrete samples were subjected to similar curing conditions as for the panels by storing the samples next to each panel. The grout samples were placed inside a plastic bag to emulate the condition of the grout inside the metal ducts, and were tested on the same day as when the panel testing occurred. The strengths of used material are summarised in Table 2.

3.3 Test setup

Two different test setups were used for testing the five panel-to-foundation connections. In the first series of experiments, where no additional axial load applied to the panels, the test setup primarily consisted of a foundation, a precast concrete panel and a horizontally mounted hydraulic actuator providing the horizontal cyclic lateral load, as shown in Figure 1a. The panels were stabilized from out-of-plane movements by two parallel H shape steel columns that were placed on each side of the panel.

In the second series of experiments a different test setup was used in order to apply axial loads to the panels during application of the lateral load. The axial load was applied through two post-tensioned tendons that were positioned on each side of the panel. The force in the tendons was adjusted during each experiment to keep the axial force to within ±5% of target. The tendons were connected to a beam that was positioned perpendicularly on top of the steel I section beam placed on the top of the panel and a pivot was used between two beams in

order to prevent application of any moments to the wall. In order to prevent panel out-of-plane movement two channel section beams were installed on each side of the panel. One end of the channel beams was connected to the strong wall and the other end was connected to a column placed at the other end of the panel. The details of the second test setup are shown in Figure 1b.

Table 2 – Properties of utilized materials (all stresses in MPa units)

Test number	Grout strength	Concrete strength	Connection reinforcement		Panel reinforcement	
			Yield stress	Ultimate stress	Yield stress	Ultimate stress
1	58	46	473	632	523	653
2	50	56	473	632	523	653
3	52	43	482	629	520	641
4	54	53	482	629	520	641
5	64	45	469	722	520	641

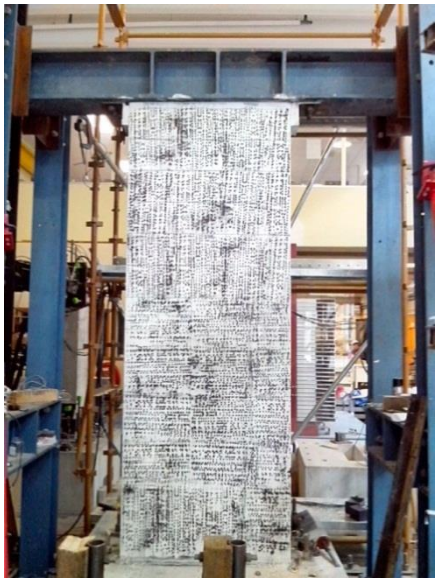

(a) Test setup without application of axial load

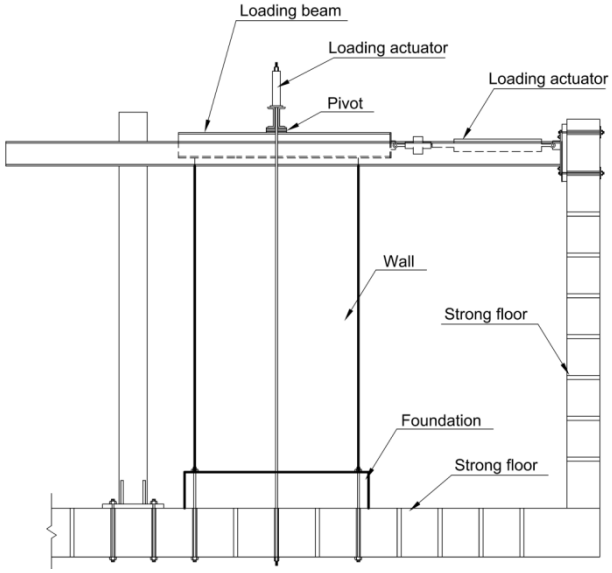

(b) Test setup with application of axial load

Fig. 2 – Test setup

3.3 Testing procedure

A loading protocol based on ACI recommendations [5] was used for reverse cyclic loading sequences, with the failure point defined as the point where the lateral force had reduced to 80% of the maximum lateral force or the stiffness had reduced to less than 10% of the initial stiffness. The applied loading started with three cycles of force-controlled loading and continued with a series of displacement-controlled loading cycles until failure. Each stage of displacement-controlled loading consisted of three cycles to the selected drift value. According to the ACI loading protocol the drift value for the next three cycles was the displacement between 5/4 times and 3/2 times the previous maximum displacement.

4. Experimental results

4.1 General response

The response of the panels varied in relation to the panel aspect ratio and application of the axial load on the panels. The crack patterns of the five tested panels are shown in Figure 3 and Figure 4. No cracks formed on Panel 1 during the first three force-controlled cycles. During the fourth cycle, a gap between the wall and foundation opened and the panel start to rock. As loading continued at a drift level of 0.15% a larger gap opened at the base of the wall and small cracks also appeared at a height of about 600 mm above the foundation where the metal ducts ended. As the lateral drift increased, the wall response was dominated by rocking at the wall-to-foundation interface and noticeable sliding also occurred at the wall base. Several small cracks occurred in the panel and at a drift level of 2% the largest crack in the wall panel at a height of 600 mm reached a width of 1.6 mm. The experiment concluded with rupturing of connection reinforcement during a cycle to 2.5% drift. No significant concrete crushing or spalling was observed in Panel 1.

Rocking and sliding also dominated the overall behaviour of Panel 2, which had a double layer of reinforcement. In all inelastic cycles, a gap opened at the wall-to-foundation joint and the panel remained undamaged, without forming any cracks or concrete spalling. The larger reinforcement content in the doubly reinforced panel significantly increased the panel flexural capacity in comparison to the connection flexural capacity. As with the previous test, panel sliding was observed during large drift cycles. This experiment concluded with rupturing of the extreme connection reinforcement at a drift level of between 2% and 2.5%.

Due to application of axial load, a different behaviour was observed in Panel 3 in comparison to Panel 1 that had the same dimensions. Rocking still dominated the overall behaviour of the panel, but less cracks formed on the panel when compared to Panel 1. The axial load prevented the panel from cracking until a drift of 0.22%. At this drift level a small crack appeared at a height of 600 mm, where the metal ducts ended. At a drift level of 0.75% a gap opened at the connection due to panel rocking, and also small cracks also appeared in the compression toe of the wall, resulting from the initiation of concrete compression failure. At the next four drift levels of 0.75%, 1.0%, 1.5% and 2.0% the length and width of cracks extended and more extensive concrete spalling was observed. In comparison with the previous two tests, less panel sliding was observed due to application of axial load to the panel that increased the friction at the connection. At the next drift level of 2.5% the strength had reduced by greater than 20% and therefore failure was defined as having occurred at this drift level. The experiment was continued by applying a drift level of 3.5% to the panel, which caused fracture of the extreme connection reinforcement.

A different response was observed in Panel 4 due to this panel having a larger aspect ratio. More extensive concrete spalling was observed in compression toes of the panel due to the larger length of the compression zone. At the second force-controlled cycle a crack formed at the wall-to-foundation interface and the panel start to rock. During the cycle to 0.33% drift, two cracks formed on each side of the panel at a height of about 500 mm and 800 mm, with widths of 0.5 mm and 0.2 mm respectively. At a drift of 0.5% these cracks extended towards the middle of the panel and intersected each other to form a single crack. In addition, the concrete of panel corner initiated to spall due to the panel flexural deformation. At a drift level of 1.5% more extensive concrete spalling occurred, which allowed the extreme metal ducts to pull out from the panel. The metal duct at the other side of the panel was pulled out from the panel at a drift of 2.0%. The more extensive flexural damage in this test in comparison with the previous three panels indicated the larger contribution of flexural deformation within the panel. At the initial stage of loading Panel 5 behaved similarly to Panel 4, with narrow distributed cracks forming on both sides of the panel. The difference between the two experiments occurred when a drift larger than 1.0% was applied to the panels. In Panel 5 less concrete spalling was observed at the corners of the panel due to the placement of additional reinforcement in the connection zone and connection reinforcement rupture occurred on both sides of the panel at a drift level of 1.5%. Less cracks formed on Panel 5 due to proper splice between panel and connection splice and the increased vertical reinforcement that supported the confining stirrups. The condition of the connections in Panel 4 and Panel 5 at the end of the test are shown in Figure 5.

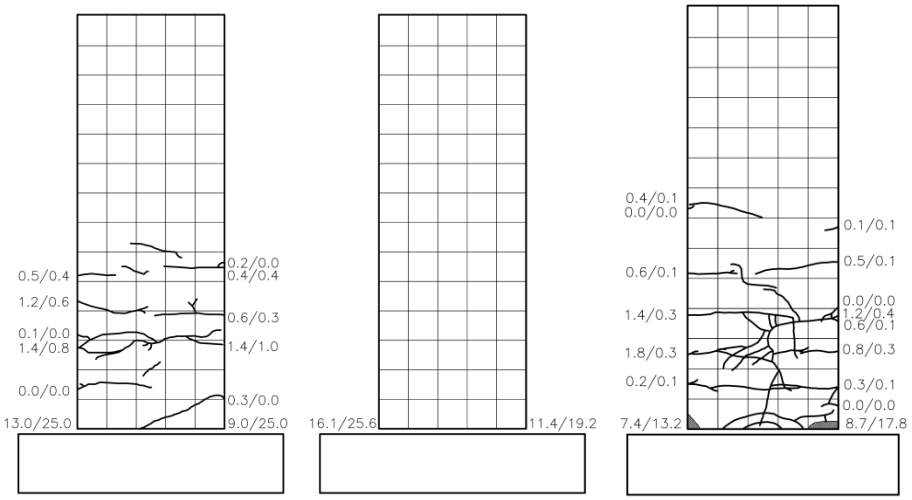

(a) Panel 1 (b) Panel 2 (c) Panel 3

Fig. 3 – Crack patterns in Panel 1 to Panel 3

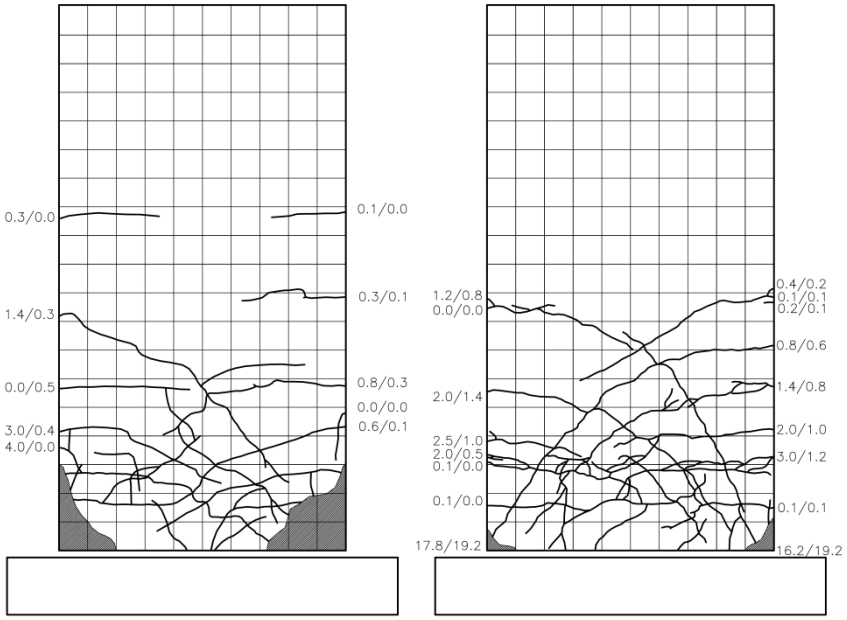

(a) Panel 4 (b) Panel 5

Fig. 4 – Crack patterns in Panel 4 and Panel 5

4.2 Force-displacement behaviour

The resultant force-displacement response for Panel 1 and Panel 2 are plotted in Figure 6. The response of the two panels was almost identical as their connection properties and failure modes were similar. During the first three forced-controlled cycles the panels exhibited an almost linear elastic behaviour and in the fourth cycle inelastic behaviour was observed due to crack formation in the panel and yielding of the connection reinforcement, causing pinching of the force-displacement response. This behaviour was due to the opening of a gap in the connection zone which reduced the panel stiffness as the moment was carried only by the reinforcement. In the next cycles when more cracks were formed in the panel and a larger gap opened at the connection further pinching of the hysteretic curves was observed. Finally both tests were completed when the

connection reinforcement ruptured, causing rapid strength degradation. The panels had almost the same maximum lateral strength of about 53 kN and at the time of bar fracture the residual panel strength was about 20% of the maximum lateral force. A drift capacity of 2% was achieved by both panels prior to failure.

(a) Panel 4 (b) Panel 5

Fig. 5 – Condition of the wall ends for Panels 4 and 5 at the end of the test

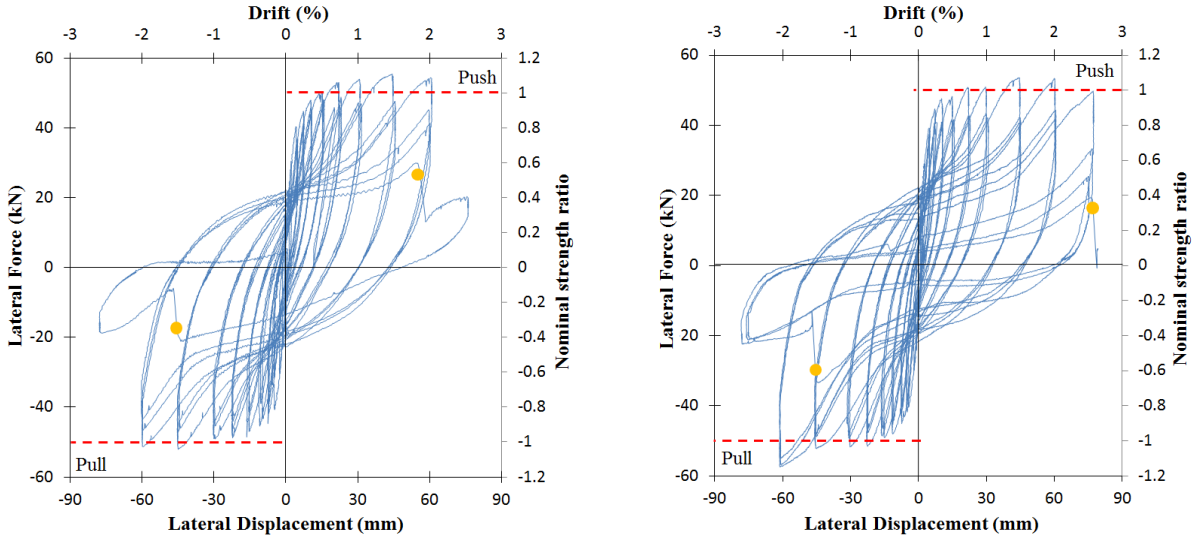

(a) Panel 1 (b) Panel 2

Fig. 6 – Hysteresis response of panels without application of axial load (● indicates bar rupture)

The force-displacement response of Panel 3 is shown in Figure 7a. During three forced-controlled cycles a linear behaviour was observed, and first yield in the connection reinforcement occurred during the fourth cycle. At larger drifts the force-displacement response started to display nonlinear behaviour, with greater residual drift caused by plastic deformation of the connection reinforcement and crack formation on the panels. The magnitude of residual drift was smaller than that observed in earlier tests due to smaller gap opening at the connection and the formation of fewer cracks in the panel. The panel lateral strength reached a maximum of 110 kN at a drift level of 2.0%. At the next drift level of 2.5% concrete more extensive cracks was formed and spalling occurred at the corners of the panel, resulting in decrement panel stiffness and a drop in lateral strength to 75 kN. The experiment was continued by applying 3.5% drift that caused fracture of the connection reinforcement. The reinforcement failure occurred at the larger drift than the previous two tests due to the smaller gap opening at the wall base and reduced deformation of the connection reinforcement. The lateral strength measured in this experiment was approximately twice the value measured in the previous two

experiments due to the application of axial load. The other difference between this test result and the earlier tests was that the unloading curve was less steeply inclined than for the previous experiments, resulting in smaller residual drifts in each cycle. In addition, there was less pinching of the force-displacement response than for the previous two tests. The reason for these changes in behaviour was attributed to the increased magnitude of applied axial load, which decreased the tensile force within the connection reinforcement and consequently the extent of plastic deformation in this reinforcement.

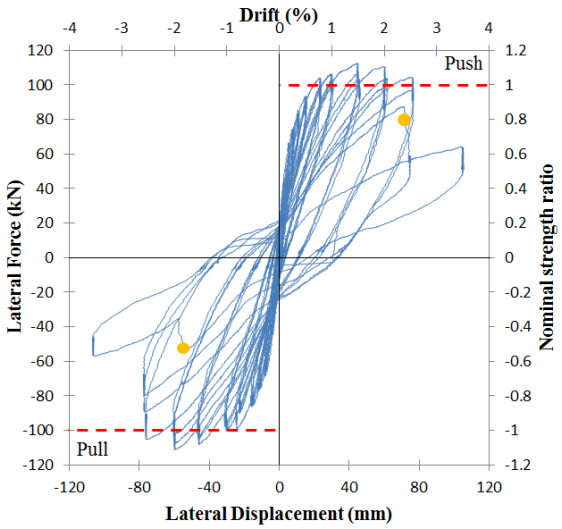

(a) Panel 3

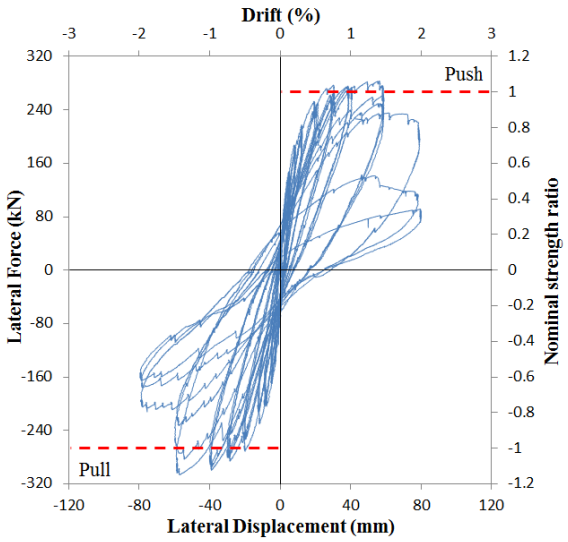

(b) Panel 4

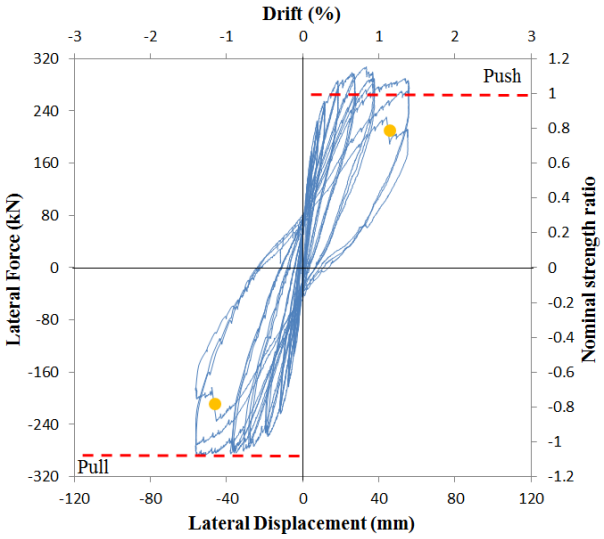

(c) Panel 5

Fig. 7 – Force-displacement response of panels with application of axial load (● indicates bar rupture)

In Figure 7b and Figure 7c the force-displacement response of Panel 4 and Panel 5 are shown. Larger lateral forces were measured in these panels when compared with the previous three experiments, due to larger panel dimensions and the greater magnitude of the axial compression load. In the drift levels of below 1.5% the Panel 4 and Panel 5 responses were almost identical, indicating that the effect of more extensive concrete spalling in Panel 4 was not significant on the load-displacement curve. The peak lateral strengths of Panel 4 and Panel 5 reached similar values of 308 kN for Panel 4 and 307 kN for Panel 5 but their corresponding drifts were different, with values of 1.5% for Panel 4 and of 1.0% for Panel 5. The reason for this different magnitude of drift at failure between the two tests was attributed to the different mode of failure in each experiment. Failure of

Panel 4 was due to progressive concrete spalling which led to the metal duct becoming disconnected from the panel, as shown in Figure 5a. In contrast the failure of Panel 5, which had more robust splices between the panel and connection reinforcement, was due to connection reinforcement fracture. Larger degradation was observed in the response of Panel 4 when compared to Panel 5 due to the formation of larger cracks and more extensive concrete spalling in Panel 4. In addition, no sudden drop in the lateral strength was observed in Panel 4 because no reinforcement rupture occurred during this test.

4.3 Deformation components

Rocking, sliding, shear and flexural deformation were the four mechanisms identified for the precast concrete panels connected to their foundation, as expected for panels subjected to in-plane lateral forces [6]. The contributions of each mechanism were obtained by displacement gauges that were installed on the panels and their connections to the foundation. The extent of panel flexural deformation was determined by measuring the curvature of panel sections. By assuming that panel cross-sections remain plane during loading the flexural deformation of the panel was obtained using the approach proposed by Hiraishi [7]. Panel shear deformations were calculated using the data from diagonal displacement gauges, again based upon a previously proposed approach [7] which accounted for flexural deformation effects on the diagonal displacement. The extent of panel rocking was computed according to the uplift measured by two displacement gauges positioned on each edges of the panel and panel sliding was measured directly by a LVDT and a displacement gauge that were positioned at the middle of the panel. The sum of the four mechanism displacements was compared with the measured displacement at the top of the panels and the difference between these two magnitudes indicated that the error of measurement was less than 10% for all seven conducted experiments. The contribution of each mechanism to the response of the five wall teats are shown in Figure 8 and Figure 9.

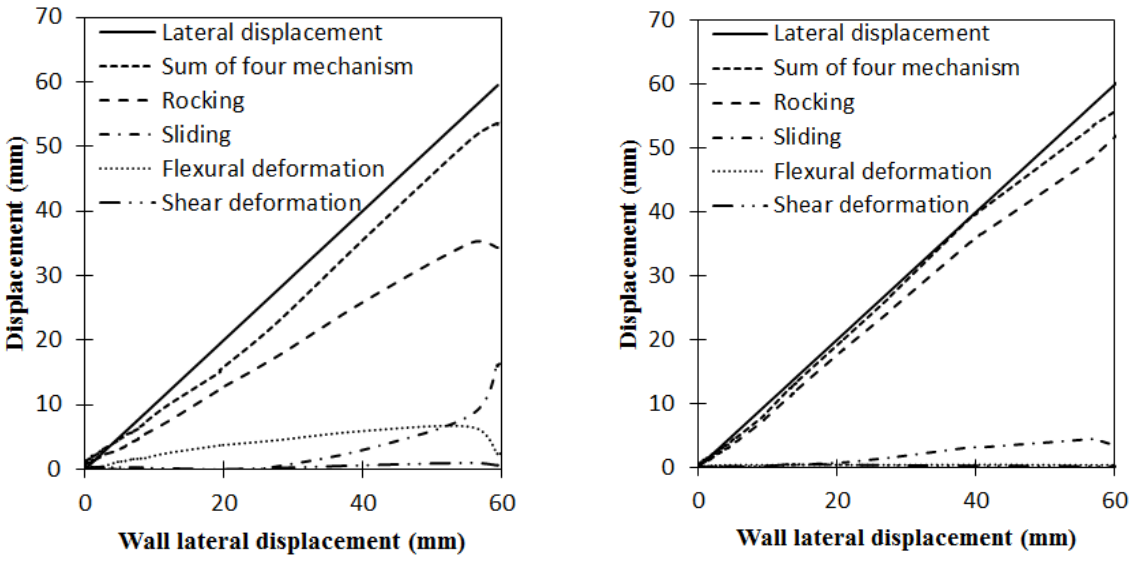

(a) Panel 1 (b) Panel 2

Fig. 8 – Contribution of deformation components for panels tested without application of axial load

In all panels except Panel 4 the overall behaviour of the panel was governed by rocking as more than 60% of the displacement at the top of the panel was due to rocking. The reason for the lower contribution of rocking in Panel 4 was attributed to the increased panel flexural deformation due to lower aspect ratio of the panel that increased the length of the compression zone. The use of additional reinforcement and confining stirrups in Panel 5 prevented extensive panel flexural cracking and concrete spalling which reduced the contribution of panel flexural deformation in comparison to Panel 4.

In Panel 1 the panel flexural deformation was approximately 15% of the overall displacement when the connection reinforcement force was below the value corresponding to yielding of the connections reinforcement. At larger drift levels, yielding of the connection reinforcement resulted in the opening of a gap in the connection and facilitated sliding of the panel. Therefore, at larger drift levels sliding displacements contributed more than

flexural displacements to the total behaviour of the panel. Shear deformation had a negligible contribution to the hysteretic behaviour of Panel 1.The contribution of rocking in Panel 2 was larger than for Panel 1 because Panel 4 had a larger thickness and greater vertical reinforcement content, which resulted in reductions both shear and flexural deformation of the panel. The largest contribution of rocking to the overall behaviour of the panels was measured in Panel 1 and Panel 2. The reason for this behaviour was the lack of axial load that facilitated panel rocking. In addition, the lower axial load limited the panel concrete spalling and consequently lessened the panel flexural deformation in comparison with other experiments. The contributions of each deformation component in Panel 3 were similar to the previous two experiments but the influence of rocking and sliding was lower because of the application of the axial load. In Panel 4 and Panel 5 the panel flexural deformations were a larger contribution of the overall response in comparison with the previous three experiments reported above. The reason for this behaviour was the larger applied axial compressive load and a larger panel length, which increased the compression force in the panel toe causing more extensive concrete spalling and increased panel deformation.

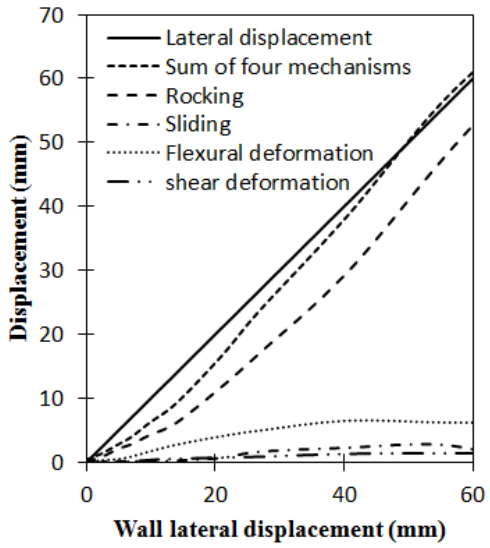

(a) Panel 3

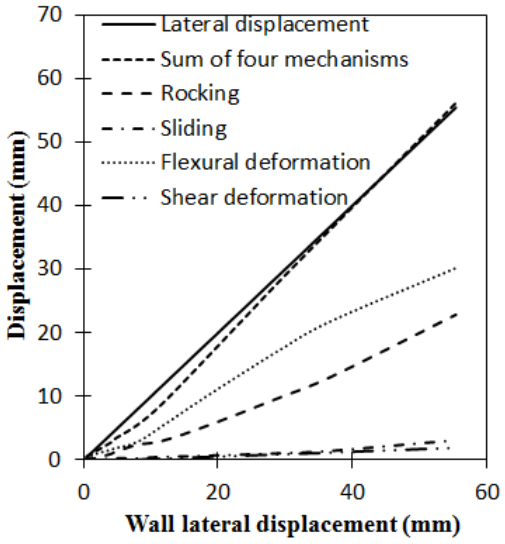

(b) Panel 4

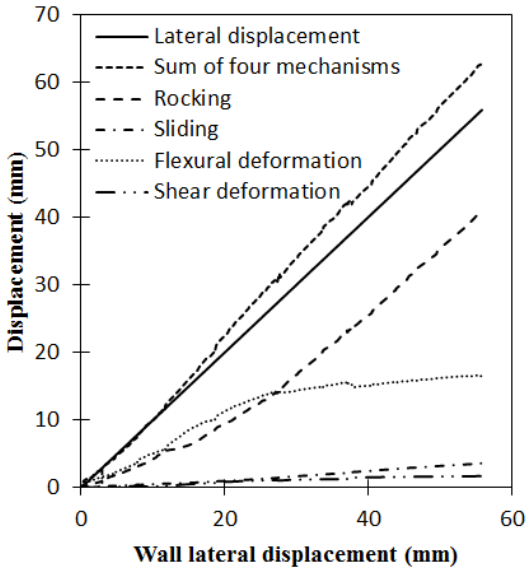

(c) Panel 5

Fig. 9 – Contribution of deformation components for panels tested with application of axial load

4.4 Energy dissipation

Equivalent viscous damping (EVD) is a parameter that is used in the displacement-based seismic design method. The EVD can be determined by:

$$\xi = \frac{A_h}{2\pi F_m \Delta_m} \quad (1)$$

Where ξ is equivalent viscous damping, A_h is the enclosed area of each cycle, F_m is maximum lateral force in a cycle, and Δ_m is the maximum displacement in a cycle. The calculated EVD for each tested panel are shown in Figure 10. The EVD of all tested panels were generally low in comparison with values obtained when testing monolithic concrete walls [8]. The reason for this response is the limited extent of plastic deformations, which mostly developed in the connection zone. Where the drift was lower than 1.5%, the EVD increased as a larger displacement was applied to the panel. This behaviour was due to more extensive damage and plastic deformations when the panel was subjected to the larger drifts. In Panel 1 to Panel 6 the EVD reached a peak value at a drift level of 1.5% and it decreased when the drift went beyond this level. This behaviour was mainly due to plastic deformation of the connection reinforcement which caused larger pinching of the force-displacement diagram.

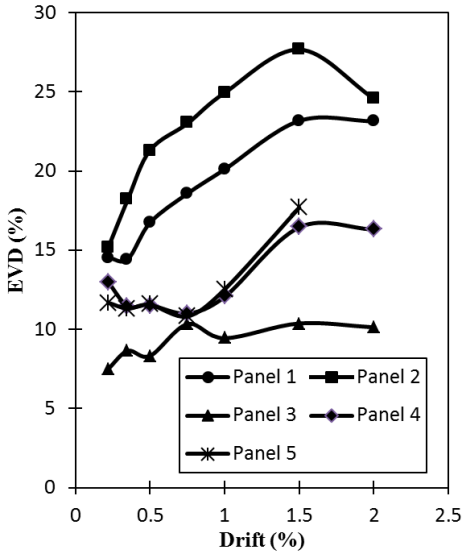

Fig. 10 – Equivalent viscous damping of each panel

Panel 1 and Panel 2 had a larger EVD than for the other three panels as no axial load was applied to these panels. The EVD of these two panels varied, with this variation being attributed to the different confinement details adopted for the connection region of each panel. It was observed that a greater level of confinement allowed the connection reinforcement to yield over a larger length, resulting in greater energy dissipation [9]. Consequently the lower EVD was measured in Panel 1 than Panel 4 because of lower thickness of Panel 1provided less confinement, resulting in a lower EVD. Panel 3 to Panel 5 had lower EVD than for previous four experiments due to application of the axial load that caused a more steeply inclined unloading curve with a thinner force-displacement diagram. Panel 3 had less EVD than for Panel 4 and Panel 5 as less damage occurred in this panel. In Panel 4 and Panel 5 more extensive concrete spalling was observed, which increased the magnitude of dissipated energy. The EVD of Panel 5 was slightly larger than for Panel 6, which was attributed to more heavily confinement of the connection.

5. Conclusions

The cyclic behaviour of precast concrete walls with grouted metal duct connections was investigated, focusing on parameters such as wall aspect ratio, axial load, and the connection splice. It was established that the

influence of connection confinement in panels with a moderate level of axial load was significant. Confinement of the splice between the panel and connection reinforcement prevented the duct from pulling out from the wall, and allowed the panel to behave in a more ductile manner than when no confinement was provided. In addition, it was observed that the application of axial load increased panel strength, and significantly decreased the equivalent viscous damping and residual drift of the panels. Generally single layer reinforced panels with confined connections had an acceptable performance.

It was found that panels with a weak connection experienced lower levels of damage and that almost all damage was concentrated in the connection at the wall base. From the observed crack patterns it was concluded that when damage was limited to the grout layer and with other parts of panels being mostly undamaged, the metal duct connections are more easily repairable after an earthquake.

It was observed that the overall force-displacement behaviour of precast concrete walls can be considered with acceptable accuracy by summing four deformation mechanisms that were rocking, sliding, shear and flexural deformation of the panel. Because all tested panels had a large aspect ratio the behaviour of the walls was dominated by rocking and flexural deformation of the panels. Panel sliding would be likely to occur at large drift levels when the connection reinforcement yielded and a gap opened between the panel and the foundation. The application of axial load to panels limited the gap opening and consequently decreased the extent of panel sliding. The influence of panel shear deformation was found to be negligible.

6. Acknowledgements

This research was funded by the Natural Hazard Research Platform (NHRP). Materials associated with the testing of walls were provided by Precast New Zealand Incorporated and Sika Ltd and their contributions are gratefully acknowledged. The authors also wish to acknowledge the contributions of Mark Byrami, Ross Reichardt, Andrew Virtue, Shane Smith, Jay Naidoo and Jerome Quenneville who were responsible for practical aspects in relation to the testing of the wall specimens in the Structures Testing Lab at the University of Auckland.

7. References

[1] Crisafulli FJ, Restrepo JI, Park R (2002): Seismic design of lightly reinforced precast concrete rectangular wall panels. *PCI Journal*. **47** (4). 104-121.

[2] PCI Industry Handbook Committee (2010): *PCI Design Handbook: Precast and Prestressed Concrete*. Prestressed Concrete Inst, 7th Edition, Chicago, IL.

[3] SESOC Interim Design Guidance (2013): *Design of conventional structural systems following the Canterbury earthquakes*. Version No.9, Structural Engineering Society of New Zealand, New Zealand.

[4] Seifi P, Henry RS, Ingham JM (2016). Panel connection details in existing New Zealand precast concrete buildings. *Bulletin of the New Zealand Society for Earthquake Engineering*. **49** (2). 190-199.

[5] ACI Innovation Task Group 5 (2008): Acceptance criteria for special unbonded post-tensioned precast structural walls based on validation testing and commentary (ACI ITG-5.1 M-07). *American Concrete Institute*, Farmington Hills, MI.

[6] Becker JM, Llorente C, Mueller P (1980): Seismic response of precast concrete walls. *Earthquake Engineering & Structural Dynamics*, **8** (6). 545-564.

[7] Hiraishi H (1984): Evaluation of shear and flexural deformation of flexural type shear walls. *Bulletin of the New Zealand National Society for Earthquake Engineering.* **17** (2). 135-144.

[8] Zhang, Y, and Zhihao W (2000): "Seismic behavior of reinforced concrete shear walls subjected to high axial loading." *ACI Structural Journal*. **97** (5). 739-750.

[9] Saatcioglu M, Razvi SR (1992): Strength and ductility of confined concrete. *Journal of Structural Engineering*, **118** (6). 1590-1607.